Assessment of Left Ventricular Perfusion, Volumes, and Motion in Mice Using Pinhole Gated SPECT

André Constantinesco, MD, PhD[1]; Philippe Choquet, PhD[1]; Laurent Monassier, MD, PhD[2]; Vincent Israel-Jost, MSc[1,3]; and Luc Mertz, PhD[1]

[1]Service de Biophysique et Médecine Nucléaire, Hôpital de Hautepierre, Strasbourg, France; [2]Institut Clinique de la Souris, Illkirch, France; and [3]Institut de Recherche Mathématique Avancée, Strasbourg, France

Quantitative functional normal data should be a prerequisite before applying SPECT in murine models of cardiac disease. Therefore, we investigated the capability of in vivo pinhole gated SPECT for establishment of a reference database for left ventricular myocardial perfusion, volumes, and motion in normal mice. **Methods:** A small-animal dedicated pinhole γ-camera with a field of view of 17 cm and a focal distance of 12 cm was used with a 1.5-mm pinhole and a 2.5-cm radius of rotation. Phantoms were designed to test spatial resolution and microvolume measurements of accuracy. Eight adult normal mice (CD1) were studied using a heated mixture of air (0.3 L/min) and 1.5%–2.5% isoflurane for anesthesia. For myocardial perfusion, 350–450 MBq of ^{99m}Tc-tetrofosmin were used in 0.15–0.25 mL. Gated acquisitions (8 or 10 time bins per cardiac cycle) were obtained using a 180° circular arc and 48 anterior projections of 300 R–R intervals. Image reconstruction was done using a specific Algebraic Reconstruction Technique (ART) cone-beam algorithm. For quantification, reconstructed images were processed using standard nuclear medicine software. **Results:** Millimetric spatial resolution and volume calibration linear relationships ($r^2 = 0.99$) in the 10- to 100-μL range were obtained in phantoms and used to scale in vivo volume values. In mice, left ventricular perfusion was lower in the apex (65% ± 6%) versus lateral (72% ± 5%), inferior (74% ± 5%), septum (75% ± 4%), and anterior (74% ± 2%) walls. The left ventricular ejection fraction was 60% ± 9%, end-diastolic volume was 50 ± 8 μL, end-systolic volume was 20 ± 6 μL, stroke volume was 29.5 ± 6 μL, and cardiac output was 9.6 ± 1.6 mL/min. Wall thickening was higher in the apex (47% ± 12%) versus lateral (30% ± 9%), inferior (33% ± 8%), septum (37% ± 10%), and anterior (33% ± 10%) walls. **Conclusion:** This work shows that in vivo pinhole gated SPECT can be used for assessment of left ventricular perfusion, volumes, and cardiac function in normal mice.

Key Words: mice; gated SPECT; myocardial perfusion; ventricular function; molecular imaging

J Nucl Med 2005; 46:1005–1011

Because of their genetic similarity to humans, mice are used as transgenic models in which genetic alterations define the disease phenotype. However, because of the small size of the animal (~30 g), noninvasive in vivo molecular imaging techniques capable of delivering morphologic and functional myocardial data in cases of cardiovascular phenotyping need to be adapted to the millimeter-sized structure of the mouse's heart and the corresponding high heart rate (~400–500 bpm). High-frequency ultrasound imaging, which is easy to handle for screening and longitudinal investigations, is able to acquire selected 2-dimensional (2D) slices in real time with high spatial and temporal resolutions well adapted for morphologic and mechanical functional data (*1*) and, more recently, 3-dimensional (3D) volumes but with less spatial and temporal resolutions (*2*). In the same way, high-magnetic-field MRI techniques are more time consuming but able to vary high spatial resolution for volumes and motion at the expense of less temporal resolution (*3*). However, these techniques lack the sensitivity for tissue functional metabolism viability. For this reason, radiotracers and nuclear imaging techniques are potentially useful (*4*). Small-animal PET systems have been developed and used for cardiac imaging in small animals but there are some intrinsic limitations due to the random walk of positrons, which, in turn, limits the finest spatial resolution between 1.2 and 2 mm (*5,6*). On the contrary, micro SPECT, based on pinhole collimators of a very small aperture and a camera small radius of rotation, offers the advantages of being capable of submillimeter or millimeter spatial resolution without too much expense in sensitivity (*7–11*). It is also obvious that cardiac nuclear imaging of mice needs a good temporal resolution if ventricular wall motion is considered. In this respect, and compared with the high sensitivity of small-animal PET, myocardial perfusion SPECT radiotracers at physiologic equilibrium permit long-time electrocardiographically (ECG) gated acquisitions due to long half-lives of the single-photon γ-emitters used (^{201}Tl, ^{99m}Tc), leading to a sufficient signal-to-noise ratio

Received Dec. 2, 2004; revision accepted Feb. 14, 2005.

For correspondence or reprints contact: André Constantinesco, MD, PhD, Service de Biophysique et Médecine Nucléaire, Centre Hospitalo-Universitaire Hautepierre, 1 Av. Molière, 67098 Strasbourg, France.

E-mail: andre.constantinesco@chru-strasbourg.fr

despite the low sensitivity due to the small aperture of the pinhole.

However, gated micro SPECT of the mouse's heart is difficult to achieve using a commercial γ-camera because of difficulties in lowering the rotation diameter and ensuring an accurate center of rotation (COR) during acquisition despite correction COR software that is used for preprocessing of the images but that is not adapted to the pixel resolution needed (*12*). Care must also be taken for mouse position, anesthesia, and temperature to ensure both a motionless and a stable heart rate during long-time acquisition (*4*). These difficulties explain why only one group, to our knowledge, has presented a study of nongated myocardial perfusion SPECT in a murine model of permanent coronary occlusion (*9*) and one case of perfusion gated SPECT (with 8 time bins per cardiac cycle) in a normal mouse, using a human stationary γ-camera and a rotating vertical mouse holder, illustrating the potential of the technique (*8*). Therefore, dedicated micro SPECT devices should be able to answer not only the technical and practical problems of in vivo routine cardiac mouse nuclear imaging but also the key question of data quantification needed for longitudinal cardiovascular phenotyping (*13*). The aim of this study was to demonstrate that a reference-quantified database of left ventricular (LV) wall perfusion distribution, ejection fraction, volumes, and motion could be obtained in a series of normal mice using ECG gated SPECT with a dedicated system and the use of standard cardiac nuclear medicine software.

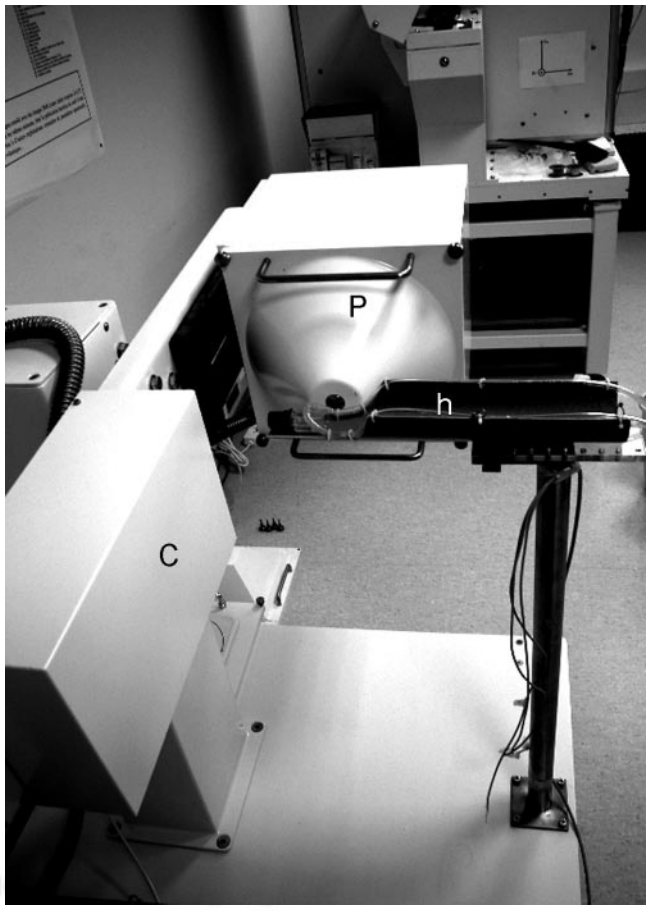

FIGURE 1. Close-up view of dedicated small-animal pinhole SPECT camera. P = pinhole collimator; C = counterweight; h = small-animal holder.

MATERIALS AND METHODS

Micro SPECT System Description and Mouse Holder

We used a small-animal single-head dedicated γ-camera (Gaede Medizinsysteme GMBH) with a 6.5-mm NaI(Tl) crystal equipped with 25 photomultipliers and a small field of view of 17 × 17 cm. The camera was equipped with a pinhole collimator of 12 cm in focal length and a lead insert of 1.5 mm in diameter. The camera and the corresponding counterweight were mounted on a rotating gantry allowing, with a reduction screw, the manual adjustment of the distance between the pinhole and the axis of rotation in a range of 1–10 cm with 0.1-mm accuracy (Fig. 1). The computer-driven circular rotation of the camera permitted testing of the accuracy of the COR, and preprocessing correction was applied on the projection images before tomographic reconstruction using the line source method as described (*10*).

We designed a 4-cm-diameter acrylic cylindric holder that keeps the mouse horizontal and that is open within the thorax to minimize, as much as possible, the radius of rotation of the camera.

Phantom Studies

To test the tomographic spatial resolution capabilities of the dedicated SPECT camera and reconstruction algorithm, we designed a phantom consisting of an acrylic cylinder with 3 series of cylindric holes of 1, 2, and 3 mm separated by 1, 2, and 3 mm, respectively, as shown in Figure 2, that were filled with ^{99m}Tc-pertechnetate. The second phantom series were phantoms to calibrate the small-volume measurement capability of the dedicated micro SPECT camera, taking into account the whole image reconstruction and quantification procedure, in the range of 10–100 μL. For this purpose, a continuously adjustable pipette, which is a digital volumeter, to set the volumes with a known accuracy and precision (2%), was used and the conical pipettes were filled with ^{99m}Tc-pertechnetate (Gilson P20 and P200). For phantoms we used nongated SPECT acquisitions whose parameters were 48 projections of 1 min in a 64 × 64 word format over an arc of 180° using the 1.5-mm pinhole and a 2.5-cm radius of rotation. After image reconstruction with our algorithm, the phantom SPECT volumes were then calculated by counting the corresponding number of voxels in axial slices encompassing the object, before multiplication by the reconstructed voxel size. Then and before the use of commercial software packages for cardiac murine image quantification (Quantitative Perfusion SPECT [QPS] and Quantitative Gated SPECT [QGS]; GE Healthcare), care was taken to adjust the scale factor needed to correct the voxel size, following the idea of Croteau et al. in rat heart gated PET (*14*), due to the geometric assumptions of these software programs adapted for human applications (*15*).

Animal Procedures, Anesthesia, ECG Gating, and Tracer Administration

Eight normal adult female mice (CD1; Institut Clinique de la Souris) weighting 27 ± 3 g were included in this study, and the French regulations concerning small-animal experimentation (authorization 67-104) were followed. One extremity of the mice

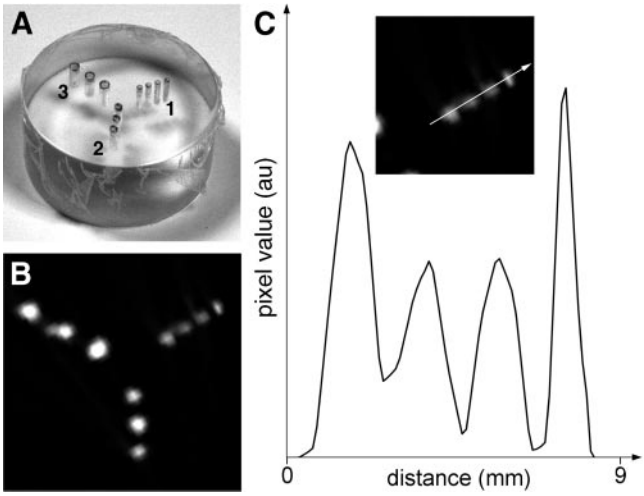

FIGURE 2. (A) Upper view of resolution phantom in which each set of cylindric holes of 1, 2, and 3 mm is separated by the same distances. (B) Corresponding reconstructed mid axial slice in which holes of 1 mm are clearly separated. (C) Activity line profile through 1-mm hot spots. au = arbitrary unit.

holder was attached to a respiratory tube connected to a small-animal anesthesia device capable of delivering a heated gas mixture (air and 1.5%–2.5% isoflurane) to keep the temperature of the animal constant during experimentation (Minerve). For ECG gating we used subcutaneous needle electrodes connected to an electrocardiograph (Physiogard RSM 784 ODAM). For the imaging modality tested in this study, we catheterized the femoral vein for intravenous administration of the radiotracer. For perfusion, 350–450 MBq of ^{99m}Tc-tetrofosmin (Myoview; GE Healthcare) were used. Care was taken to minimize, as much as possible, the volume of injected tracers around 0.15–0.25 mL to avoid significant changes in the whole blood volume of the mice.

Gated SPECT Acquisition Parameters

Myocardial perfusion acquisitions were started 15–20 min after tracer administration to ensure a better contrast of heart to soft tissue due to hepatobiliary clearance of the tracer. The radius of rotation of the camera was adjusted at 2.5 cm corresponding to a zoom factor of 4.8. A 20% window centered on the 140-keV photoelectric peak of the ^{99m}Tc was used. With mice in the supine position, a circular anterior, 48-projection step-and-shoot acquisition over 180° with 64 × 64 word images from the left lateral to the right lateral side of the thorax was used. We registered 300 cardiac beats for each projection in a forward–backward mode with a 20% temporal window of the mean R–R time. In 5 cases we registered 8 time bins per cardiac cycle, whereas in 3 cases we registered 10 time bins per cardiac cycle. At the end of the examination, data were transferred to a G4 personal computer (Apple Computers) for image reconstruction.

Image Reconstruction Technique

The image reconstruction method used in this study has been described (*16,17*). Briefly, it consisted of calculating the exact geometric spot corresponding to each image projection of the object voxels taking into account the cylindric geometry induced by the rotation of the γ-camera around the animal. Thus, we used a polar discretization, the voxels being laid out on concentric rings. Deconvolution is then automatically achieved by solving the linear system given by the projection equations using the Algebraic Reconstruction Technique (ART) algorithm also taking into account the intrinsic resolution of the γ-camera, the effective diameter of the pinhole, the spatial variation of sensitivity, and a uniform attenuation. The number and size of the object voxels are predefined as the field of view encompassing the object. Therefore, the number of voxels and dimensions of the field of view permit predetermination of the isotropic tomographic spatial resolution expressed in mm/pixel. Diffusion was not considered but could be introduced in the algorithm (*18*). Before reconstruction, image projections were corrected for radioactive decay of ^{99m}Tc due to long-time acquisition.

Myocardial Perfusion and Functional Image Analysis

For each perfusion gated SPECT acquisition and after completion of reconstruction of axial slices, the whole isotropic data cube was resliced according to the mouse heart axis to obtain short-axis, vertical long-axis, and horizontal long-axis slices using commercial nuclear imaging software (Mirage, version 5.048; Segami). For quantification of LV perfusion, volumes, and motion, gated short-axis slices were then analyzed with the same commercial nuclear medicine software packages as previously (QPS and QGS). These clinical packages use cardiac perfusion SPECT short-axis slices in gated and ungated modes as input data for computing the inner and outer LV walls and valve plane. Relative LV wall perfusion (normalized to the hottest pixel) and several functional parameters are then automatically derived, including end-systolic and end-diastolic volumes, enabling determination of ejection fraction, stroke volume, and regional wall thickening (*15*).

RESULTS

Phantom Studies, Reconstructed Pixel Resolution, and Spatial Resolution

For the resolution phantom as well as for myocardial perfusion images in mice, we used a reconstructed field of view of 30 mm, leading to a pixel resolution of 0.47 mm and a corresponding reconstructed voxel of 0.1 mm^3. For spatial resolution, Figure 2 shows that 1-mm holes of the spatial resolution phantom can be easily separated, leading to a millimeter spatial resolution. For microvolume calibration, we obtained a linear relationship between measured volumes by SPECT and reference volumes ($y = 0.974x + 3.680$) (Figure 3), with $r^2 = 0.99$. There is a slight 3.7-μL overestimation of the measured SPECT volumes, probably due to the image reconstruction and volume quantification process and statistical noise.

Gated Myocardial Perfusion Images of Mice

Figure 4 shows a typical example of time evolution of an axial midventricular slice through systole and diastole corresponding to the 10 time bins defined at acquisition in this particular case. Changes in the shape of the left ventricle are clearly visible, and the right ventricle could also be distinguished in the 8 mice of the series—however, with less contrast than the left ventricle. Figure 5 shows a typical time-summed midventricular short-axis slice in which, again, left and right ventricular cavities and corresponding walls can be easily identified.

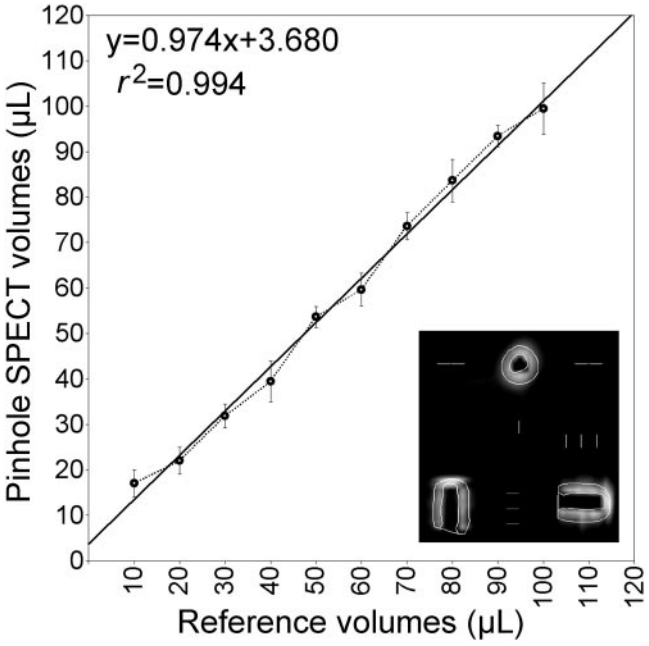

FIGURE 3. Linear relationship between measured volumes after pinhole SPECT reconstruction and corresponding calibrated values. SPECT volumes were obtained by multiplying the reconstructed voxel size by their number after counting pixels in each short-axis slice image using a 15% threshold of the maximum pixel. For each reference volume, 5 different pinhole SPECT acquisitions were obtained in 5 different filled pipettes, and the corresponding mean value is represented as a black circle. Because QGS and QPS analyses are based on automatic detection of LV inner and outer walls, we verified that inner and outer limits of a static micro LV volume are accurately matched using QPS by simulating a ventricular cavity of known volume in the set of 1 micropipette short-axis image by forcing to zero a known number of pixels. Inner and outer walls of this ventricular model were correctly detected by QPS, leading to an accurate measurement of the simulated ventricular volume as illustrated in the inset (35 µL measured using QPS vs. calibrated 30 µL).

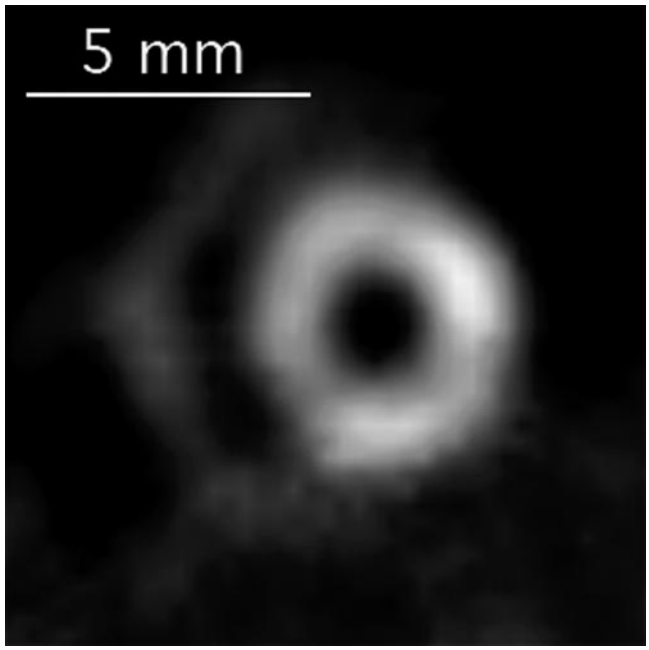

FIGURE 5. Midventricular time-summed perfusion short-axis slice of mouse of Figure 4, in which left and right ventricular cavities and walls are clearly visible.

Quantification of LV Perfusion, Volumes, and Motion in Mice

After processing by the QPS software applied to the time-summed short, vertical, and horizontal slices, the left myocardial perfusion mean values (relative to the hottest pixel of the LV polar plot of each case as usual in nuclear cardiology) of the wall segments analyzed in this study (Table 1), shown in Figure 6, are remarkably similar for the anterior, lateral, inferior, and septum walls (between 72% and 75%) and the apex exhibits a slight (65%) hypoperfusion. For all segments, we observed a low SD of the relative perfusion values. For the LV kinetics, heart rate was 331 ± 35 bpm during acquisition, and Figure 7 illustrates the systolic and diastolic 3D QGS-computed LV views of a typical case and corresponding LV ejection fraction curve. Table 2 lists mean values and corresponding SDs of the LV ejection fraction, end-diastolic and end-systolic volumes, stroke volume, and cardiac output after scaling by the linear volume calibration relationship measured in phantoms. Wall motion can also be derived from QGS analysis and expressed in the percentage of thickening. The apex has the highest percentage of thickening (47% ± 12%), whereas the lateral wall has 30% ± 9%, the inferior wall has 33% ± 8%, the septum wall has 37% ± 10%, and the anterior wall has 33% ± 10%.

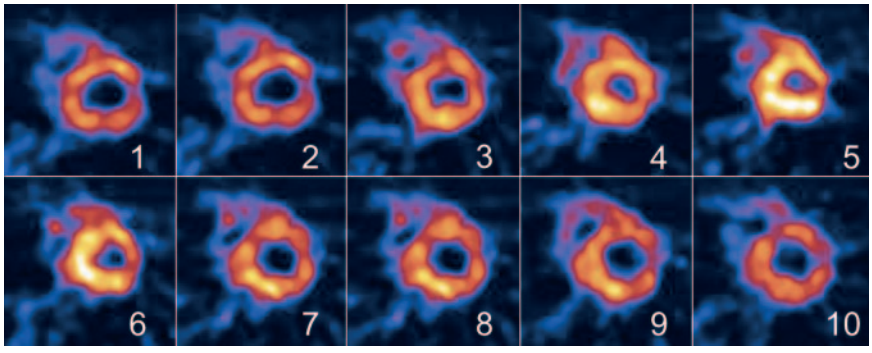

FIGURE 4. Ten time phases of a midventricular perfusion axial slice of a mouse throughout systole and diastole. Note changes in ventricular cavities (left and even right) during contraction and relaxation.

TABLE 1
Mean Values ± SD of Relative Wall Perfusion and Thickening of Left Ventricle for 8 Mice of Series

LV wall segment	Relative perfusion (%)	Relative thickening (%)
Apex	65 ± 6	47 ± 12
Lateral	72 ± 5	29 ± 9
Inferior	74 ± 5	33 ± 8
Septum	75 ± 4	37 ± 10
Anterior	74 ± 2	33 ± 10

DISCUSSION

Influence of Anesthesia on Cardiovascular Function of Mice

Mouse hemodynamics are highly sensitive to anesthesia (*4*); therefore, reference LV parameters should preferably be obtained in conscious animals because LV function is altered under 250 bpm, as was demonstrated in a recent study using echography (*19*). However, SPECT cannot be done without anesthesia. Isoflurane, as other anesthetics, decreases the heart rate and, therefore, particular attention was made to keep the heart rate as high and stable as possible during our experiments. As a consequence, care must be taken when comparing functional LV parameters obtained with different anesthetics and examination conditions due to different imaging modalities.

Comparison with Other Studies

LV global perfusion in BALB/c mice was also studied with nongated SPECT applied to a murine model of coronary occlusion by permanent ligation of the left anterior descending coronary artery with ^{99m}Tc-sestamibi as the tracer and with a similar spatial resolution of 1.1 mm (*9*). Our results can be compared only with the control group ($n = 6$) of this study, in which we observed an apical relative hypoperfusion of 60%, which corresponds to the value we measured and which could be influenced by the thin apical wall thickness and corresponding partial-volume effects, as gallbladder activity was reported to be reduced by injecting cholecystokinin (0.1 μg/g) before SPECT acquisition (*9*). To our knowledge, there are no comparable gated SPECT studies with regard to the LV volumes, ejection fraction, and cardiac output; however, our results are in the same range of those obtained, in equivalent normal mice series and anesthetic conditions, using high-field MRI (*3,20*) or echography for ejection fraction, stroke volume, and cardiac output (*1,2*). Moreover, gated SPECT also permitted—to our knowledge, for the first time—a quantitative analysis of LV wall thickening, a finding that requires further comparative MRI and echography studies to test its accuracy.

Quantification

One of the advantages of gated SPECT shown in this study is that quantification of mouse LV parameters, after reconstruction and reorientation, was obtained through validated automatic image software analysis that is used routinely in human nuclear cardiology. This means that, considering the volume calibration linear relationship enabling the appropriate scale factor has been done, reproducibility and intra- or interobserver variability of the technique are those currently accepted in human clinical routine. Under these conditions, perfusion gated SPECT should now permit longitudinal follow-up and pharmacologic stress studies of LV perfusion and kinetics in mouse models of cardiovascular disease, as has been demonstrated in rats for PET and SPECT (*14,21*).

Spatial and Time Resolutions, Acquisition Time, and Sensitivity

Pinhole gated SPECT is a true 3D imaging method leading to isotropic voxels as 3D echography (*2*) but contrary to MRI, which uses 2D contiguous slices due to gated imaging strategies (*3,20*), and 2D echography, which is limited to specific slices (*1*). Spatial resolution of micro SPECT was 1 mm in this study and is limited by sensitivity correlated with the pinhole diameter and the organ distance to the pinhole (*16*). However, we demonstrated that both ventricles were clearly visible. Submillimeter spatial resolution (0.5 mm) should probably be achievable in the future with specific multipinhole techniques (*22,23*). An accurate analysis of LV kinetics requires a good time resolution of the R–R interval. In this respect, we showed in this study that 10 time bins per cardiac cycle is achievable. Preliminary results in our laboratory indicate that 16 time bins are possible, which are to be compared with 15–25 for high-field MRI depending on the imaging sequence and, obviously, the real time

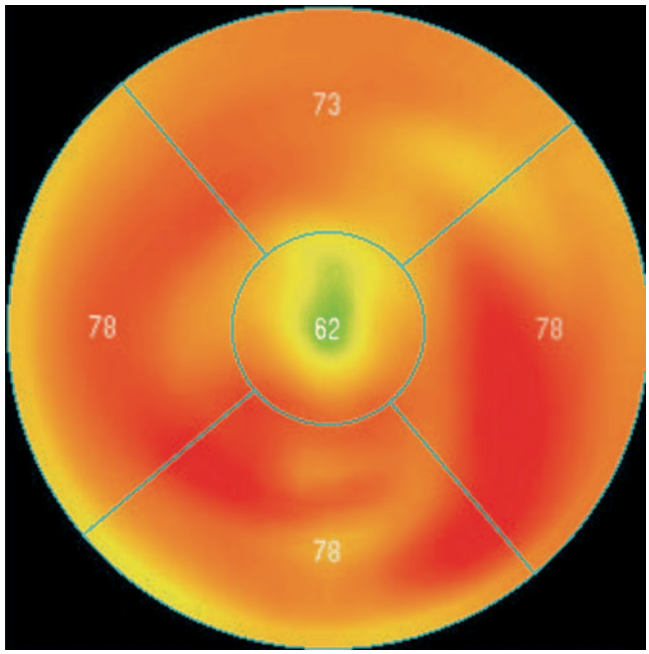

FIGURE 6. LV perfusion bull's eye polar plot of a mouse derived from QPS analysis and showing wall segmentation. Apical relative hypoperfusion can be observed. 62, 73, and 78 refer to average percentage of the maximum.

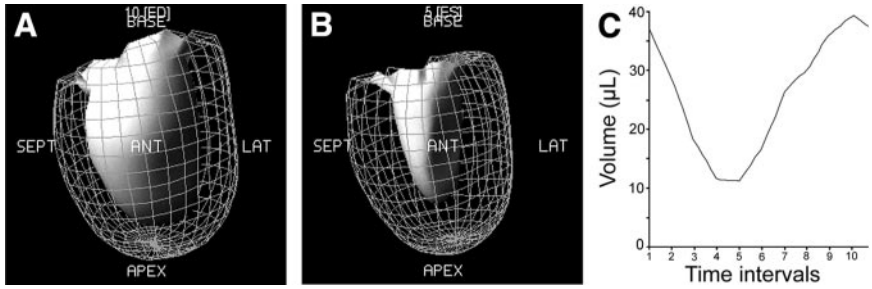

FIGURE 7. Computed 3D LV contours of a mouse derived from QGS analysis in systole (A) and diastole (B) allowing for ejection fraction curve (C), volumes, and wall thickening measurement. ED = end diastole; ES = end systole; SEPT = septal; ANT = anterior; LAT = lateral.

for echography (*1,2,19*). However, one needs to keep in mind that perfusion gated SPECT is able to deliver mean values of LV parameters measured in about 300 cardiac cycles compared with other imaging modalities (echography, high-field MRI), in which time resolution is better but only a few consecutive cycles are analyzed. One of the drawbacks of gated SPECT is the long acquisition time, around 1 h as for MRI, depending on the number of detectors and the diameter of the pinhole (*4,8,9,12*). Nevertheless, this long acquisition time could be decreased using the multipinhole or the coded aperture approaches, which increase SPECT sensitivity without degrading spatial resolution (*22,23*).

Amount of Radioactivity and Volume of Injected Tracer Used

Another limitation of SPECT in mice is the amount of radioactivity needed for a good contrast-to-noise ratio. Contrary to intuition, this amount—which is similar to that used for humans despite important differences in body mass between mouse and man—is due to the size of image voxels, which corresponds to the mouse scale (*4*). At the high specific activities used, 2 issues remain unanswered for mice. The first is to be certain that the radiopharmaceutical causes no pharmacologic effect but still acts as a tracer, as was demonstrated for PET in rats (*24*). The second is related to mouse organs and whole-body absorbed doses during SPECT, which could influence the outcome of mice in the case of longitudinal examinations. Finally, this high amount of radioactivity is needed in a minimal volume compared with the mouse blood volume. Our injected volumes were in the same range of those used by other investigators in an ungated perfusion study in BALB/c mice (*9*). However, care must be taken to slowly inject the tracer in about 5–10 s.

TABLE 2
Mean Values ± SD of Ejection Fraction, Volumes, and Cardiac Output for 8 Mice of Series

Parameter	Value
Heart rate (bpm)	331 ± 35
Time bins/R–R	8 (n = 5), 10 (n = 3)
EF (%)	60 ± 9
EDV (µL)	50 ± 8
ESV (µL)	20 ± 6
SV (µL)	29.5 ± 6
CO (mL/min)	9.6 ± 1.6

EF = LV ejection fraction (EDV − ESV/ESV); EDV = LV end-diastolic volume; ESV = LV end-systolic volume; SV = LV stroke volume (EDV − ESV); CO = cardiac output (SV × heart rate).

Sources of Image Blur

Finally, movement of the mice during SPECT must be suppressed to minimize sources of image blur. As we used ECG gating in this study, respiratory movements induce a millimeter-scale uncontrolled supplementary motion of the heart. This could be artificially controlled by adding a respiratory gating but at the expense of increasing acquisition time (*4,25*).

CONCLUSION

In this study we demonstrated that, after careful calibration and using standard nuclear medicine software, perfusion ECG gated SPECT in mice permits quantification of LV volumes and motion, enabling establishment of a functional normal database, which should be a mandatory step before using the method in murine models of cardiovascular disease.

ACKNOWLEDGMENTS

The authors acknowledge GE Healthcare and CIS-Bio Schering (Paris, France) for their support and Lahcen Elfertak for expertise in management of the mice.

REFERENCES

1. Collins K, Korcarz C, Lang R. Use of echocardiography for the phenotypic assessment of genetically altered mice. *Physiol Genomics.* 2003;13:227–239.
2. Dawson D, Lygate CA, Saunders J, et al. Quantitative 3-dimensional echocardiography for accurate and rapid cardiac phenotype characterization in mice. *Circulation.* 2004;110:1632–1637.
3. Wiesman F, Ruff J, Dienesch C, et al. Cardiovascular phenotype characterization in mice by high resolution magnetic resonance imaging. *MAGMA.* 2000;11:10–15.
4. Green MV, Seidel J, Vaquero JJ, Jagoda E, Lee I, Eckelman WC. High resolution PET, SPECT and projection imaging in small animals. *Comput Med Imaging Graph.* 2001;25:79–86.
5. Chatziioannou AF, Cherry SR, Shao Y, et al. Performance evaluation of microPET: a high resolution lutetium oxyorthosilicate PET scanner for animal imaging. *J Nucl Med.* 1999;40:1164–1175.
6. Schelbert H, Inubushi M, Ross R. PET imaging in small animals. *J Nucl Cardiol.* 2003;10:513–520.
7. Beekman FJ, McElroy DP, Berger F, Gambhir SS, Hoffman EJ, Cherry SR. Towards in vivo nuclear microscopy: iodine-125 imaging in mice using micropinholes. *Eur J Nucl Med.* 2002;29:933–938.

8. Wu M, Tang R, Gao D, Ido A, O'Connell J, Hasegawa B. ECG-gated pinhole SPECT in mice with millimeter spatial resolution. *IEEE Trans Nucl Sci.* 2000; 47:1218–1221.
9. Wu M, Gao D, Sievers R, Lee R, Hasegawa B, Dae M. Pinhole single photon emission computed tomography for myocardial perfusion imaging of mice. *J Am Coll Cardiol.* 2003;42:576–582.
10. Ogawa K, Kawade T, Nakamura K, Kubo A, Ichihara T. Ultra high resolution pinhole SPECT for animal study. *IEEE Trans Nucl Sci.* 1998;45:3122–3126.
11. Acton P, Choi S, Plössl K, Fung H. Quantification of dopamine transporters in the mouse brain using ultra-high resolution single photon emission tomography. *Eur J Nucl Med.* 2002;29:691–698.
12. Ishizu K, Mukai T, Yonekura Y, et al. Ultra high resolution SPECT system using four pinhole collimators for small animal studies. *J Nucl Med.* 1995;36:2282–2289.
13. MacDonald L, Patt B, Iwanczyk J, et al. Pinhole SPECT of mice using the Lumagem gamma camera. *IEEE Trans Nucl Sci.* 2000;47:1163–1167.
14. Croteau E, Bénard F, Cadorette J, et al. Quantitative gated PET for the assessment of left ventricular function in small animals. *J Nucl Med.* 2003;44:1655–1661.
15. Germano G, Berman DS. On the accuracy and reproducibility of quantitative gated myocardial perfusion SPECT. *J Nucl Med.* 1999;40:810–813.
16. Israel-Jost V, Monassier L, Choquet Ph, Blondet C, Sonnendrücker E, Constantinesco A. Feasibility of rat myocardial gated SPECT using a standard gamma camera [in French]. *ITBM-RBM.* 2004;25:15–22.
17. Constantinesco A, Choquet P, Monassier L, Israel-Jost V, Elfertak L, Sonnendrücker E. A micro-SPECT imaging pilot study of myocardial perfusion in mice [in French]. *Med Nucl.* 2004;28:163–168.
18. Li J, Jaszczak RJ, Greer KL, Coleman RE. A filtered backprojection algorithm for pinhole SPECT with a displaced centre of rotation. *Phys Med Biol.* 1994;39:165–176.
19. Seznec H, Simon D, Monassier L, et al. Idebedone delays the onset of cardiac functional alteration without correction of Fe-S enzymes deficit in a mouse model for friedreich ataxia. *Hum Mol Genet.* 2004;13:1017–1024.
20. Schneider JE, Cassidy PJ, Lygate C, et al. Fast, high resolution in vivo cine magnetic resonance imaging in normal and failing mouse hearts on a vertical 11.7 T system. *J Magn Reson Imaging.* 2003;18:691–701.
21. Camici P. Gated PET and ventricular volume. *J Nucl Med.* 2003;44:1662.
22. Beekman FJ, Vastenhouw B. Design and simulation of a high resolution stationary SPECT system for small animals. *Phys Med Biol.* 2004;49:4579–4592.
23. Schramm NU, Ebel G, Engeland U, Schurrat T, Behe M, Behr TM. High resolution SPECT using multipinhole collimation. *IEEE Trans Nucl Sci.* 2003; 50:315–320.
24. Jagoda EM, Vaquero J, Green MV, Eckelman WC. Experiment assessment of mass effects in the rat: implications for small animal PET imaging. *Nucl Med Biol.* 2004;31:771–779.
25. Cassidy PJ, Schneider JE, Grieve SM, Lygate C, Neubauer S, Clarke K. Assessment of motion gating strategies for mouse magnetic resonance at high magnetic fields. *J Magn Reson Imaging.* 2004;19:229–237.